Journal of Membrane Science 677 (2023) 121633

Contents lists available at ScienceDirect

Journal of Membrane Science

journal homepage: www.elsevier.com/locate/memsci

Design of a process development workflow and control strategy for single-pass tangential flow filtration and implementation for integrated and continuous biomanufacturing

Shashi Malladi *, Michael J. Coolbaugh, Crystal Thomas, Sushmitha Krishnan, Chad T. Varner, Jason Walther, Kevin P. Brower

Mammalian Platform, Global CMC Development, Sanofi, Framingham, MA, 01701, USA

ARTICLE INFO

Keywords:
Integrated and continuous biomanufacturing
Single-pass tangential flow filtration
Robust control
Commercial-scale
Biologics

ABSTRACT

Integrated and continuous biomanufacturing (ICB) offers several advantages compared to traditional batch methods, prompting the development of novel technologies and infrastructure for the implementation of ICB in the biopharmaceutical sector. However, most of the advancements have been in the early stages of the purification process, with relatively fewer advancements in the final filtration steps. This work focuses on some of the last major unit operations of a traditional bioprocess: ultrafiltration and diafiltration. Our proposed technological solution involves robust control algorithms for (1) precisely maintaining consistent protein concentration in single-pass ultrafiltration (SP-UF) and (2) achieving the targeted buffer exchange in single-pass diafiltration (SP-DF). Specifically, we adopted an integrated experimental, modeling, and simulation approach to develop a robust process understanding of SP-UF/SP-DF operations via semi-empirical maximum permeate flux models. These models were employed in the optimization of key design variables such as the filter area and the development of control strategies. Finally, we demonstrate the applicability of our proposed solution by operating a single-pass tangential flow filtration (SP-TFF) system in an integrated and continuous manner for six days. We believe that this work is instrumental for the successful realization of SP-UF/SP-DF operations in both batch and ICB processes.

1. Introduction

In the last few years, the biopharmaceutical industry has seen a paradigm shift from traditional batch processing towards integrated and continuous biomanufacturing (ICB) [1–4]. The underlying factors driving this shift are due to the increased necessity to achieve process intensification and implement agile manufacturing resulting from the need to respond to varying material needs and diverse modalities in the pipeline. From a process intensification perspective, recent advances have facilitated increased cell densities in fed batch and perfusion reactors resulting in higher product volumes and titers [5–11]. These productivity gains constrain the downstream operations, necessitating greater flexibility in their design and processing capabilities in a cost-effective manner. Thus, ICB is favored for both fed-batch and perfusion bioreactors due to its inherent process intensification benefits such as reduced facility footprint, compatibility with single-use technologies, consistent and homogenous product quality, potential for modularity and universality, and reduced capital and operating costs [3, 12–14]. Furthermore, the biopharmaceutical sector is increasingly adopting lean and agile manufacturing practices to respond rapidly to fluctuating market demands arising from unexpected conditions such as a pandemic and stiff competition from biosimilars/generic drug products [15]. In this aspect, an ICB process offers the needed flexibility and enables the industry to position itself better for unforeseen circumstances.

Although ICB offers numerous benefits, its implementation is not trivial and efforts have been made to develop (i) process understanding, (ii) predictive modeling capabilities, (iii) implementation of process analytical technologies (PAT), and (iv) high-fidelity unit-level and integrated-level process control for all the unit operations in the

Abbreviations: SP-TFF, Single-pass Tangential Flow Filtration; SP-UF, Single-pass Ultrafiltration; SP-DF, Single-pass Diafiltration; ICB, Integrated and Continuous Biomanufacturing.

* Corresponding author.
E-mail address: shashi.malladi@sanofi.com (S. Malladi).

https://doi.org/10.1016/j.memsci.2023.121633
Received 19 February 2023; Received in revised form 30 March 2023; Accepted 3 April 2023
Available online 10 April 2023

purification train [16–18]. Most of the prior ICB efforts have primarily focused on developing a strategy for operating the chromatography operations [15,19,20] or virus inactivation step(s) [21,22] of the purification train in a continuous manner. Crucial downstream operations such as ultrafiltration (UF) and diafiltration (DF), which are employed for the concentration of process intermediates and drug substances [23], and for the buffer exchange of therapeutics [24], respectively, have been studied to a lesser extent and thus are the focus of the current work.

One of the key requirements for operating UF and DF in a continuous manner is the need to employ single-pass tangential flow filtration (SP-TFF) compared to the traditional tangential flow filtration (TFF) system. In recent years, SP-TFF has gained prominence compared to traditional TFF in both batch and continuous processes due to several reasons. First, it allows continuous concentration and buffer exchange of the protein solution in one filter pass. Second, given the recent advancements with increasing productivity and titer of bioreactors, SP-TFF facilitates handling of higher process volumes, unlike traditional TFF, thereby eliminating a potential bottleneck for the downstream purification operations [25]. Besides the above, traditional TFF possesses other limitations such as (i) high shear forces acting on the proteins during each pass through the pump head and filter, (ii) a constantly changing system due to the volume reduction with time leading to potential variability in product attributes, (iii) mixing and foaming issues, and (iv) low product recovery due to large holdup volumes [26–28]. All these limitations have led to the increased adoption of SP-TFF as it is effective in reducing the processing volumes by inline concentration or by instantaneously processing the material, which would lead to reduced facility footprints and thereby increased cost savings [25,26,29–31].

Thus, SP-TFF, due to its applicability in both batch and continuous processes [32–34], has garnered a growing interest in different applications. For example, Arunkumar et al. [30] used Pellicon 2 SP-TFF cassettes to perform a 10-fold concentration of cell culture harvest, which reduced the volume to be processed in the downstream operations. Jabra et al. [35] and Casey et al. [29] used SP-TFF modules for the inline concentration of a monoclonal antibody (mAb) solution to produce a drug substance (DS) of 100 and 200 g/L, respectively. Pall Corporation used a 4-in series combination of their Cadence SP-TFF cassettes (0.065 m^2 total membrane area) to achieve a 4–5x volumetric concentration factor (VCF) of the feed stream prior to loading onto a membrane chromatography column [36]. Rucker-Pezzini et al. [37] demonstrated continuous DF by connecting three SP-TFF modules in series, where the feed is concentrated and subsequently diluted with DF buffer to match the initial feed concentration. Nambiar et al. [24] and Jabra et al. [35] optimized the buffer usage by introducing DF buffer at the last SP-DF module and using the permeate of a module as the buffer to the preceding module, which provided 99–99.9% buffer exchange. Tan et al. [38] used 3D-printed single-pass UF/DF modules for simultaneous concentration by a factor of 4.6 and diafiltration, which reduced the salt concentration by 47%. Lastly, Yehl et al. [39] demonstrated SP-TFF using 1.9 m^2 Optiflux F200NR hollow fiber cartridges to achieve 10-fold concentration of the feed solution. Recently, Coolbaugh et al. [33] demonstrated integrated ultrafiltration of 8–10 g/L feed solution up to 65 $\pm$ 5 g/L and its diafiltration using SP-TFF Pall in-line concentrators and Sartocon SP-DF filters, respectively.

Besides experimental work, several modeling studies have also focused on elucidating the operating mechanisms of SP-TFF systems. Kaiser et al. [40] performed CFD modeling to identify the optimal operating conditions as a function of applied transmembrane pressure (TMP), velocity, and concentration profiles. However, their model did not consider concentration polarization effects, which play an important role in high protein concentrations. Thakur et al. [41] determined the effects of different filter configurations on the permeate flux by considering membrane resistance, concentration polarization, and mass transfer effects. Similarly, Huter et al. [42] used single SP-TFF cassettes to predict the permeate flux taking mass transfer and fluid dynamics effects into consideration. Jabra et al. [35] improved an earlier model, which predicted the permeate flux using protein-protein interactions and mass transfer of the protein solution [43], to include viscosity effects and variation in the concentration and flowrate along the length of SP-TFF cassettes.

While the above outlined works deepened our understanding of the performance of SP-TFF under various conditions, operating SP-TFF in an integrated and continuous format requires robust process controllers, as well. Generally, in any continuous process, disturbances in either the upstream or downstream operations can lead to upsets in the process of interest and high-fidelity controllers are needed to minimize the effects of such disturbances. For example, in the case of SP-TFF, some of the disturbances can be variations in harvest, equipment failure, pressure buildup in the flow lines etc. In addition, continuous processes typically operate for prolonged periods thereby necessitating steps to minimize fouling of SP-TFF membranes. There have been a few studies that have attempted to overcome these challenges by implementing control strategies. Casey et al. [29] and Thakur et al. [44], in their recent works implemented PAT-based flow ratio controllers to obtain a range of VCF (2 – 25x) by empirically determining the performance of the SP-TFF filters under different feed conditions. Additionally, Thakur et al. [44], incorporated automated cleaning and buffer flush of the membranes in their SP-TFF operations to handle membrane fouling. However, in an integrated and continuous SP-TFF operation running for an extended period, having additional steps to handle fouling, cleaning and buffer flush of the membranes can lead to intermittent pauses of the continuous operation, which might be inefficient. Thus, strategies that prevent membrane fouling are essential to develop an efficient integrated and continuous SP-TFF system. Besides the empirical determination of SP-TFF filter performance, hybrid modeling approaches such as resistance in series [41,45,46], osmotic [43,47], stagnant film and boundary layer models [42], and computational fluid dynamics (CFD) [40,48] have been employed for estimating VCF as a function of feed and process parameters. Despite their ability to predict the permeate flux and achieve the target concentration, generalizing these models to different molecules might be challenging and thus, employing them directly for robust process control of a continuous process is not readily feasible.

In this regard, our work provides a step-by-step approach for implementing a robust SP-TFF operation in either batch or continuous format. We propose a novel control strategy that prevents membrane fouling and maintains the target process and product attributes. Specifically, we describe a bottom-up framework (see Fig. 1a) for (i) developing a fundamental understanding of the SP-TFF operation, (ii) developing maximum permeate flux models that are generalizable, (iii) evaluating performance and filter sizing, and (iv) developing a robust control strategy. (It should be noted that SP-TFF, here, refers to both single-pass ultrafiltration (SP-UF), and single-pass diafiltration (SP-DF) operations). We also demonstrate the effectiveness of our framework by implementing it for a commercial scale continuous SP-TFF operation. This approach can also be employed in other kinds of biomanufacturing processes (e.g., batch or cyclic batch).

2. Theory

2.1. SP-TFF versus traditional TFF

One of the main differences between traditional TFF and SP-TFF is in the number of passes of feed solution. Generally, in traditional TFF, the feed solution undergoes multiple passes (see Fig. 1a) through the filter to concentrate the protein solution and/or achieve complete buffer exchange. This is because the filters used in traditional TFF typically allow higher feed fluxes (~300 LMH) resulting in increased sweeping rates and shorter residence time thereby requiring multiple passes [49]. On the other hand, in SP-TFF, the desired amount of protein concentration or buffer exchange occurs in a single pass (Fig. 1b) either by modulating the TMP or increasing the residence time within the filter, which is achieved either by (i) reducing the feed flowrate, (ii) using a staged

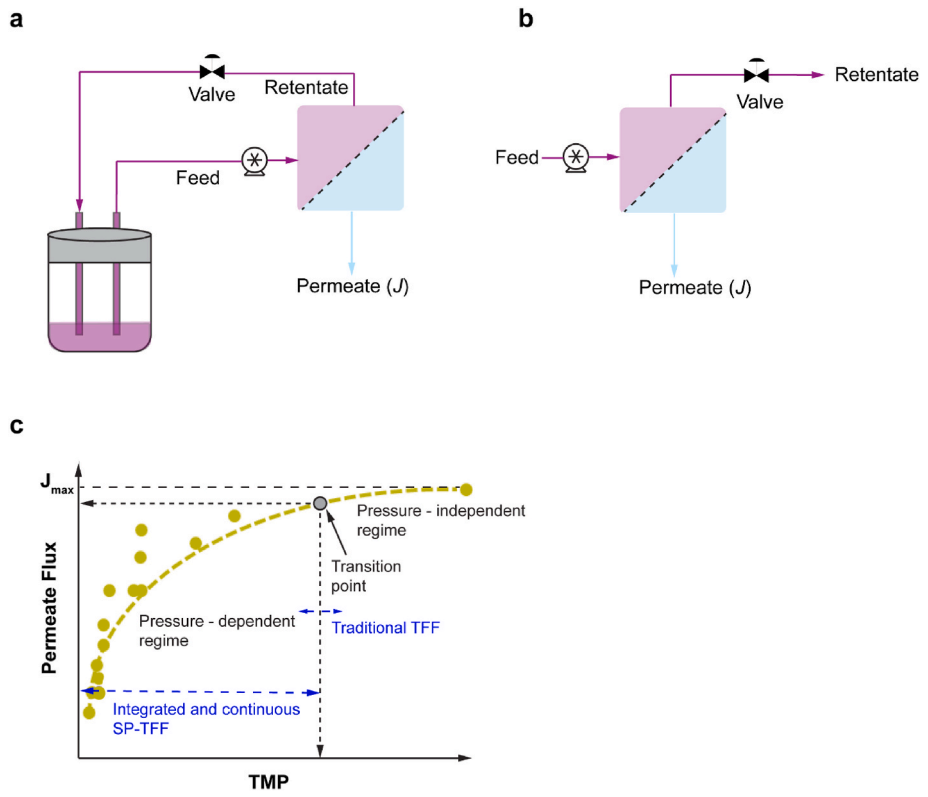

Fig. 1. Schematic of a) traditional TFF and b) SP-TFF setup. c) Representative permeate flux versus TMP plot for TFF operations.

configuration of filters that increases the path length, or (iii) using combinations of these approaches. Despite the above difference, both SP-TFF and traditional TFF are pressure-driven filtration systems with the same operating mechanism. For example, Da Costa et al. [50] and Jabra et al. [35], have developed models relating the permeate flux with TMP, feed concentration, and feed flux, and have discussed the operating mechanism under low and high TMP values. Furthermore, the mode of operation for traditional TFF and SP-TFF is defined based on the permeate flux versus the TMP profile (see Fig. 1c), which commonly has two distinct regimes – denoted as pressure-dependent and pressure-independent – separated by a transition point [51,52]. In the pressure-dependent regime, permeate flux is membrane-limited and increases with TMP whereas in the pressure-independent regime, the permeate flux is limited by mass transfer and the effect of TMP on permeate flux is negligible. In general, both traditional TFF and SP-TFF are operated in the pressure-dependent regime to prevent concentration polarization and gel layer formation, which decreases the maximum flux over time [53,54]. Table 1 provides an overview of the differences between traditional TFF and integrated and continuous SP-TFF.

Table 1
Overview of Traditional TFF and Integrated and continuous SP-TFF.

Properties	Traditional TFF	Integrated and continuous SP-TFF
Feed passes through filter	Multiple [51]	Single [29,55]
Feed concentration	Constant before the first pass and increases in the subsequent passes [56]	May vary prior to first pass itself depending on the upstream operations [26,56]
Operating regime in permeate flux vs TMP curve	Near the transition point in the pressure-dependent regime [53,54]	Below the transition point, in the pressure-dependent regime i.e., $(J < J_{max})$ [53,54]
Applied TMP	Constant to maximize permeate flux [57,58]	Variable to achieve a target permeate flux

3. Materials and methods

In this work, we have proposed a step-by-step approach (Fig. 2) for realizing an integrated and continuous SP-TFF operation. The first step involved gaining a fundamental understanding of the effects of variations in feed parameters on process performance using batch SP-TFF experiments. For this purpose, different values of feed flux and feed concentration, which were representative of the commercial-scale SP-TFF operations, were chosen and the permeate flux vs TMP profile was generated for each of them. In the second step, models relating the maximum permeate flux (J_{max}) to the feed parameters were developed using these flux-TMP profiles. In the final step, these models were employed to (1) identify the optimal filter sizing for the expected range of feed parameters and (2) define the controller operating limits during the process automation.

It should also be noted that in this manuscript, the feed and permeate flowrates are normalized by the filter area and are referred to as the feed flux and permeate flux, respectively, with units L/m^2/h (LMH). This normalization allows translation of the results to other identical filter geometries.

3.1. Batch SP-UF and SP-DF experiments for model development

In these experiments, the feed was an IgG4 molecule in an acetate buffer, which was purified by standard monoclonal antibody (mAb) purification steps – protein A chromatography, viral inactivation,

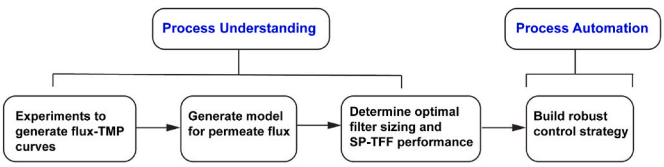

Fig. 2. Workflow for the development of SP-TFF operations.

polishing chromatography, and viral filtration. The process development experiments for batch SP-UF were performed using 2 × 0.1 m^2 SP-UF filters (30 kDa molecular weight cut-off (MWCO), Pellicon capsule with Ultracel membrane, C-screen) connected in series. For batch SP-DF, a 0.22 m^2 prototype SP-DF cassette (Hydrosart membrane, 30 kDa MWCO), provided by Sartorius, was employed. In both these systems, as shown in Fig. 3a and b, the feed was fed by a peristaltic pump (Watson Marlow) and the TMP was systematically controlled using a back pressure regulator (Equilibar, Precision Fluid Control) on the retentate stream. Additionally, for batch SP-DF, the DF buffer flowrate was controlled using a peristaltic pump (Watson Marlow) and matched with the permeate flowrate to prevent any change in concentration during the diafiltration process. To conserve material, in the case of SP-UF, the retentate and the permeate streams were recirculated into the feed vessel while for SP-DF, only the retentate stream was recirculated to prevent dilution of the feed. Independent inline single-use pressure sensors (Pendotech), single-use flowmeters (Levitronix), UV flowcells (Pendotech), and refractive index (RI) flowcells (mPath IoR, Pall Corporation) were installed on the feed, retentate, and the permeate streams to monitor the real-time pressure, flowrates, and concentrations, respectively. The RI values were converted to concentration using an in-house model. At the end of each experiment, the filter was flushed with at least 1 L of deionized (DI) water, soaked in 0.5 M sodium hydroxide (NaOH) for 2 h, and either the post-polishing or DF buffer was introduced. Buffer permeabilities were measured prior to each experiment.

3.2. Integrated and continuous SP-UF and SP-DF operations

To achieve integrated and continuous SP-UF and SP-DF operations, the SP-UF was divided into two steps (SP-UF1 and SP-UF2) with an intermediate SP-DF step (Fig. 4). The main reason for this architecture i.e., SP-UF1 – SP-DF – SP-UF2 was driven by prior process development experiments (data not shown). From these experiments, it was determined that the optimal concentration for diafiltration of the molecule considered in this work was 75 g/L. However, the expected concentration post UF and DF operations was 175 g/L, and this necessitated splitting the SP-UF operations into SP-UF1 and SP-UF2 with an intermediate SP-DF step. Specifically, the protein was first concentrated to 75 g/L in SP-UF1 followed by diafiltration at 75 g/L. Subsequently, the protein was concentrated to the expected final value of 175 g/L in SP-UF2. Although the SP-TFF operations are sequential, they are integrated using controllers to ensure continuous concentration and buffer exchange of the protein solution without intermediate surge vessels. Based on the results discussed in the next section, it is to be noted that the approach developed in this work is highly flexible and allows adopting other configurations (e.g., SP-UF – SP-DF or SP-DF – SP-UF) as well depending on the specific needs of a molecule.

3.2.1. Feed for integrated and continuous operation

Chinese Hamster Ovary (CHO) cells were cultured for 11 days in a perfusion bioreactor to produce the targeted recombinant IgG4 monoclonal antibody with a titer of 2.5 g/L at around 2 reactor volumes per day (RV/day). The clarified harvest was purified using the steps outlined by Coolbaugh et al. [33] to obtain 8.5–13.5 g/L protein solution, which was the feed for the SP-UF1 operation.

3.2.2. Integrated and continuous SP-UF1

As seen in Fig. 4, the protein solution in the surge vessel (Cercell) was pumped using a quaternary diaphragm pump (Quattroflow Fluid Systems, QF 150S, PSG Germany GmbH) to the inlet of the first of the 2 × 0.5 m^2 SP-UF1 filters (30 kDa MWCO, Pellicon capsule with Ultracel membrane, C-screen) connected in series. The volumetric flowrate of the feed stream was adjusted automatically using a level-controller on the surge vessel. Subsequently, the retentate stream from the first SP-UF1 filter was fed to the inlet of the second SP-UF1 filter. A back pressure regulator on the retentate stream of the second SP-UF1 filter systematically varied the TMP to increase the permeate flux and concentrated the protein solution to 75 g/L. This stream was fed continuously to the downstream SP-DF operation via a centrifugal pump (PuraLev i100SU, Levitronix Technologies Inc.).

3.2.3. Integrated and continuous SP-DF

The SP-DF operation involved the continuous exchange of the starting buffer of the concentrated protein solution from SP-UF1 with 5 diavolumes (DVs) of DF buffer. As shown in Fig. 4, to achieve buffer exchange, the concentrated protein solution was fed continuously (via the previously mentioned centrifugal pump) to the inlet of a 1.7 m^2 prototype SP-DF cassette (Hydrosart membrane, 30 kDa MWCO, Sartorius). Simultaneously, a peristaltic pump (Watson Marlow Inc.) fed the DF buffer at a volumetric flowrate equivalent to 5 DVs (5 times the feed flowrate) based on the inline flowrate measurement of the feed stream. The continuous SP-DF operation was designed in such a way that the rate at which the DF buffer was added into the system was equal to the rate at which the permeate was removed from the system. In addition, a back pressure regulator was installed on the retentate stream of the SP-DF filter to maintain the permeate flux by modulating the TMP. These two control elements ensured buffer exchange without altering the concentration. Finally, the SP-DF retentate stream was constantly fed to the next ultrafiltration unit (SP-UF2) using a centrifugal pump.

3.2.4. Integrated and continuous SP-UF2

In this final SP-UF2 operation, buffer-exchanged recombinant protein from the SP-DF step was further concentrated from 75 g/L to 175 g/L using a 0.5 m^2 ultrafiltration filter (30 kDa MWCO, Pellicon capsule with Ultracel membrane, C-screen, see Fig. 4). The inline sensors, and the operating principle were the same as in SP-UF1. Following this, the concentrated retentate stream was directed by a centrifugal pump to the downstream formulation operation.

3.3. Control strategy for integrated and continuous SP-UF and SP-DF operations

For the integrated and continuous SP-UF and SP-DF operations, control algorithms were implemented in Emerson's DeltaV Distributed Control Systems. The real-time values from the inline sensors were collected and stored in a PI data historian (OSIsoft). For the SP-UF1 and

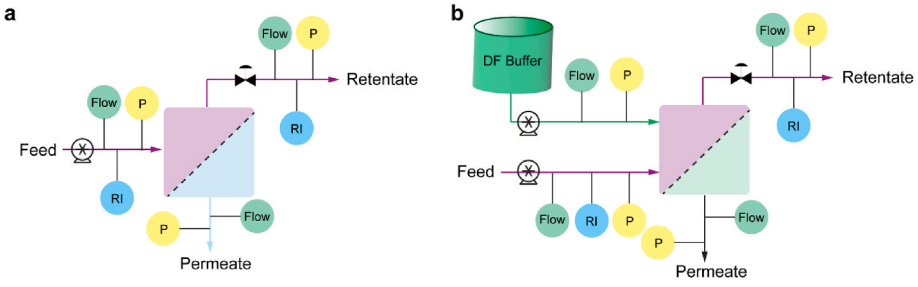

Fig. 3. Illustration of the experimental setups for a) batch SP-UF and b) batch SP-DF model development runs.

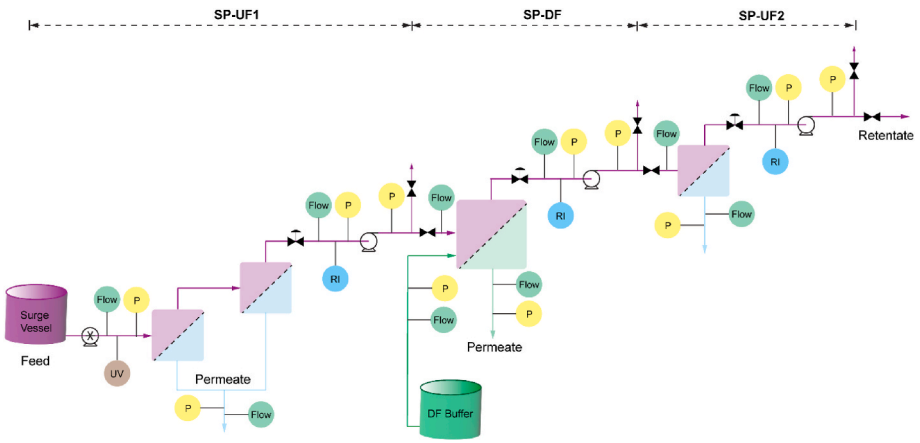

Fig. 4. Schematic overview of the integrated and continuous SP-UF1, SP-DF, and SP-UF2 operations. The inline flowmeters (represented as Flow), pressure sensors (represented as P), and refractive index (RI) and UV sensors in the various streams measure the real-time flowrate, pressure, and the concentration values, respectively. The valve pairs at the end of each operation provide alternative paths to the retentate stream—either to the downstream operation or to diversion.

SP-UF2 operations, a concentration controller was implemented to maintain consistent retentate concentration (see Fig. 5a). This was achieved by modulating the TMP on the retentate stream using a back pressure regulator based on the feed and permeate flux, and the feed and retentate concentration, measured in real-time using inline sensors. Integrated and continuous SP-DF operation was achieved using two controllers: a concentration controller (as described above) and a buffer-addition controller for ensuring fixed volumetric addition of buffer to feed, i.e., the desired DVs. The volumetric flowrate of the DF buffer was calculated in real time based on the feed and the permeate flowrates through the SP-DF cassette, which were used to dynamically adjust the set point to the peristaltic pump to vary the buffer addition rate (see Fig. 5b). Both controllers worked in synergy to ensure robust control and operation of SP-DF in an integrated and continuous format.

4. Results and discussion

Our proposed step-by-step workflow (see Fig. 2) for developing an integrated and continuous SP-TFF operation involves (i) developing a fundamental understanding of the operation, (ii) developing maximum permeate flux models, (iii) evaluating performance and filter sizing, and iv) developing robust control strategies. As it is desirable to perform integrated and continuous SP-TFF operations in the pressure-dependent regime (i.e., $J < J_{max}$), having models for J_{max} as a function of feed parameters (flux and concentration) would provide valuable insight about the potential design and operating conditions. To determine J_{max} and build the subsequent models, batch SP-UF and batch SP-DF experiments, as discussed below, were performed.

4.1. Batch SP-UF and SP-DF experiments for model development

In these experiments, permeate flux-TMP profiles were generated for varying feed concentrations (at constant feed flux) and varying feed fluxes (at constant feed concentration). The values of feed flux and feed concentration were chosen to be representative of the potential conditions for integrated and continuous SP-UF1 (concentration: 5–15 g/L, flux: 6–12 LMH), SP-UF2 (concentration: 50–80 g/L, flux: 2–4 LMH), and SP-DF (concentration: 55–75 g/L, flux: 2–4 LMH) operations. In each of the experiments, the TMP was systematically increased using a back pressure regulator on the retentate stream until a stable permeate flux was obtained. While in an ideal scenario the TMP could be increased as needed to improve the permeate flux, in some cases, it was observed that increasing the TMP beyond a certain value resulted in unsteady operations and fluctuating permeate flux. In such scenarios, the experiments were terminated and the permeate flux obtained at an earlier TMP value, in which a steady state operation was still observed, was taken as the maximum permeate flux. A summary of the feed parameters along with the experimental measurements are provided in Table 2.

Table 2
Summary of the of batch SP-TFF feed conditions and the experimental measurements.

	Batch SP-UF1	Batch SP-DF	Batch SP-UF2
Feed concentration (g/L)	5–15	55–75	50–80
Feed Flux (LMH)	6–12	2–4	2–4
Maximum Permeate Flux (LMH)	4.2–10.6	4.3–8.5	1.1–3.4
TMP at Maximum Permeate Flux (psi)	1.2–2.6	4.4–22	0.5–3.2

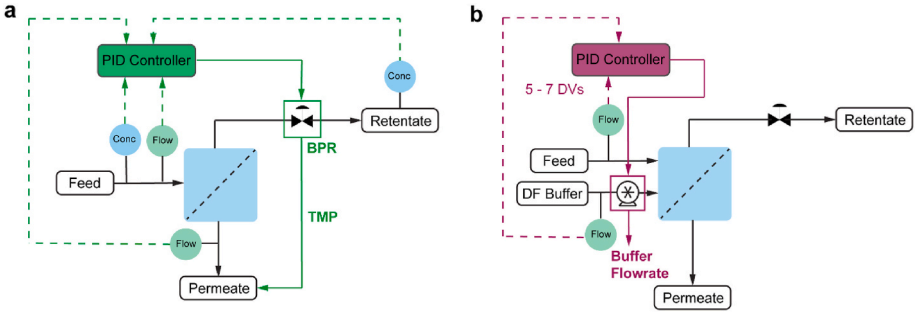

Fig. 5. Schematic of a) the concentration controller implemented for integrated and continuous SP-UF and SP-DF operations and b) the buffer addition controller for SP-DF operation.

As seen in Fig. 6a–d and Fig. 7a–b, the permeate flux increased with increasing TMP (pressure-dependent or membrane-limited regime) up to the transition point, beyond which, TMP had negligible impact (pressure-independent or mass transfer-limited regime). Additionally, for a given TMP, the permeate flux decreased with increasing concentration due to the higher mass transfer resistance at the membrane surface (Fig. 6a–b and Fig. 7a). Thus, as the feed concentration increases, higher TMPs are needed to achieve the same permeate flux. Conversely, with increasing feed flux, the permeate flux increased due to higher convective mass transfer rate or sweeping at the membrane surface (Fig. 6c–d and Fig. 7b). This higher sweeping rate minimizes the growth of the gel layer once a steady state is established. However, under these conditions, a staged filter configuration may be needed to achieve the desired concentration factor (i.e., ratio of retentate to feed concentration) or number of DVs. Similar observations were made in prior work [24,35] wherein higher feed fluxes increased the permeate fluxes through the filters.

The maximum permeate flux (J_{max}) obtained from all these studies is shown in Figs. 6e and 7c. Interestingly, the increasing feed concentration has a marginal impact on J_{max} compared to that of feed flux. This behavior can potentially be attributed to the thickness of gel layer, which imparts resistance to the permeate flux and has a stronger dependence on the feed flux than concentration. Lastly, the relationship between J_{max} (LMH) and the feed parameters for SP-UF1/SP-UF2 (equation (1)) and SP-DF (equation (2)) was found to be:

$$J_{max} = -3.28 - 0.16 * \ln C_{feed} + 3.64 * \sqrt{Q_{feed}} \quad (1)$$

$$J_{max} = 18.8 - 4.45 * \ln C_{feed} + 2.48 * \sqrt{Q_{feed}} \quad (2)$$

where C_{feed} is the feed concentration (g/L) and Q_{feed} (LMH) is the feed flux. It should be noted that the above correlations are semi-empirical and were obtained by fitting to the experimental data using multiple linear regression. Therefore, they are valid only in the range of feed flux and concentration studied here, in the described units for each factor. Though the numerical constants in the above equations are specific to the molecule used in this work, the functional form of the equation would be transferable to other molecules as well. Moreover, the predictions from the model are in good agreement with the experimental values as demonstrated by its goodness of fit (Figs. 6f and 7d), and the logarithmic and square root dependence on feed concentration and feed flux, respectively, are consistent with prior works [35,50]. Finally, these models, as described above, were employed in the next step to determine SP-TFF performance and filter sizing.

4.2. Optimal filter sizing determination

The key parameters that affect an integrated and continuous SP-UF and SP-DF operations are the feed flux and feed concentration, the filter area, and the TMP. The feed parameters are governed by the upstream operation, and they may vary in real-time due to process upsets. In response, the SP-UF and SP-DF TMP is also modulated simultaneously to accommodate the effects of such process disturbances. The only parameter that cannot be adjusted dynamically is the filter area and thus, it would have to be chosen such that it is appropriate for all possible operating conditions. In this regard, the J_{max} models shown in equations (1) and (2) and the required permeate flowrate (based on operation mass balance), were used to determine the minimum required filter area, accounting for the variability in inlet parameters. As an example, the simulation procedure adopted for SP-DF is as follows:

1) In the first step, a range of feed flowrates (0.4–1.7 L/h) and feed concentrations (50–75 g/L) were considered.
2) In the next step, the flowrate and concentration values were altered by adding random noises sampled from a Gaussian distribution with zero mean and 30% variance that corresponds to a maximum possible upstream disturbance. Furthermore, the feed parameters were perturbed to understand the impact of variability from the upstream process on the expected maximum permeate flux and the potential operating window for the integrated operation.
3) Finally, for each combination of flowrate and concentration values, the developed J_{max} model in equation (2) and the required permeate flowrate via mass balance were used to calculate the filter area with the DVs being kept constant at 5.

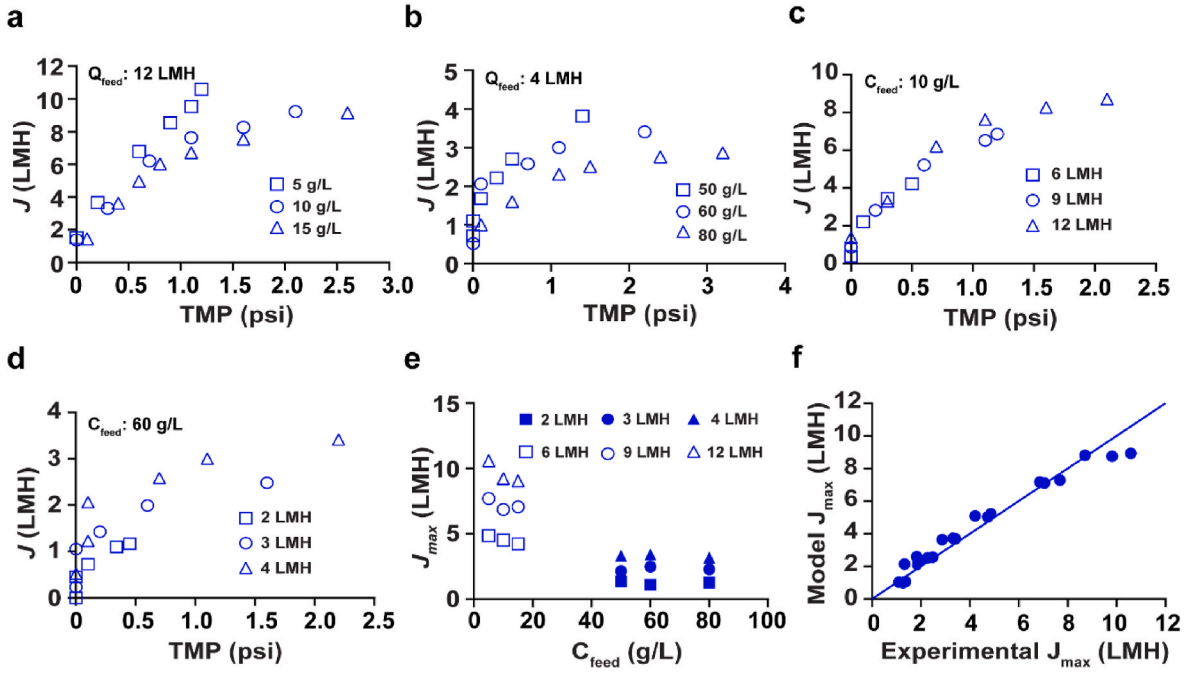

Fig. 6. Summary of the batch SP-UF results. Permeate fluxes as a function of TMP for varying feed concentrations (panels a and b) and varying feed fluxes (panels c and d) for SP-UF1 and SP-UF2. e) Summary of the maximum permeate flux as a function of feed concentration. f) Evaluation of goodness of fit for SP-UF (equation (1)).

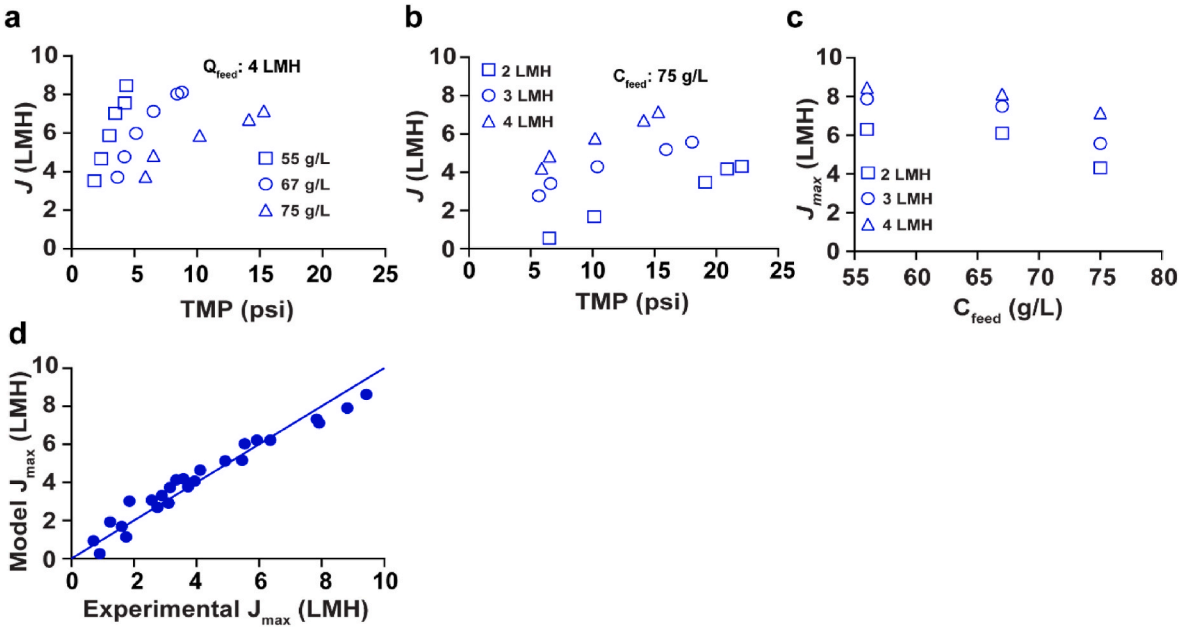

Fig. 7. Summary of the batch SP-DF results. Permeate flux as a function of TMP for a) varying feed concentrations and b) varying feed fluxes. c) Summary of the maximum permeate flux as a function of feed concentration. d) Evaluation of goodness of fit for SP-DF (equation (2)).

Fig. 8 shows the minimum required filter area such that 5 DVs of buffer exchange is achieved at all feed conditions (including the disturbances from upstream operations). Since the mass flux is constant for an integrated and continuous process (i.e., no accumulation of feed within the SP-DF unit), for the SP-DF operation, the lower bound of the filter area (~0.8 m^2) was obtained from the lowest feed concentration (or highest feed flowrate) condition. Specifically, the lowest feed concentration or highest feed flowrate condition corresponds to highest permeate flux and selecting a filter area at that condition will ensure that 5 DVs of buffer exchange will be at least achieved in all feed condition. On the contrary, if the filter area was obtained based on the lowest permeate flux condition (i.e., from highest feed concentration and lowest flowrate), employing it for relatively higher feed flowrates and lower feed concentrations would lead to lesser than 5 DVs of buffer exchange. In any case, it must be remembered that employing a very large filter area, when compared to the calculated lower bound, will reduce the flux significantly thereby preventing flow through the filter. Thus, based on the above lower bound and accounting for the available sizes (filter membranes are manufactured only in discrete sizes), a 1.7 m^2 filter was implemented to achieve minimum 5 DVs of buffer exchange for the integrated and continuous SP-DF operation. Similar simulations for SP-UF1 yielded the required minimum filter area of 0.2 m^2 (see Fig. S2) for the feed flowrates between 3 and 6.1 L/h and feed concentrations between 5 and 15 g/L.

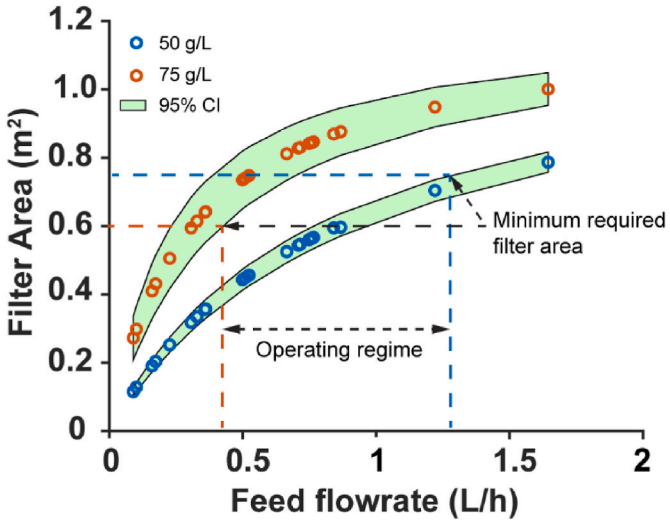

Fig. 8. Minimum required filter area for SP-DF as a function of feed flowrate at two different concentrations (50 and 75 g/L) for 30% variance in feed parameters.

4.3. *Demonstration of integrated and continuous SP-UF1, SP-DF and SP-UF2 at commercial scale*

Using the process understanding described in the preceding sections, and the process automation and control strategy outlined in section 3.3, an integrated and continuous SP-TFF operation was implemented on a commercial scale. It should be noted that the entire process consists of three sequential operations: SP-UF1, SP-DF, and SP-UF2, which are discussed in detail below. A summary of the key input parameters (feed concentration) and the process performance metrics are provided in Table 3.

4.3.1. *Integrated and continuous SP-UF1 and SP-UF2*

In both SP-UF1 and SP-UF2, a concentration controller, shown in Fig. 5a, was employed to maintain the retentate concentration at a desired value. In SP-UF1, a setpoint of 75 g/L was provided as an input, and the feed solution with a varying concentration between 5 and 15 g/L was continuously concentrated to an intermediate value of 74.5 ± 1.3 g/L (mean ± 1 S.D.) and maintained for a period of 6 days (see Fig. 9a).

Table 3
Summary of integrated and continuous SP-TFF performance at commercial scale.

	SP-UF1	SP-DF	SP-UF2
Feed concentration (g/L)	5–15	74.5 ± 1.3	76.5 ± 0.8
Retentate Concentration (g/L)	74.5 ± 1.3	76.5 ± 0.8	175.2 ± 0.5
Retentate Concentration Set Point (g/L)	75	75	175
Diavolumes	–	5.3 ± 0.1	–
Diavolumes Set Point	–	5	–
J/TMP (LMH/psi)	0.6–0.7	3.7–5.8	0.2–0.5

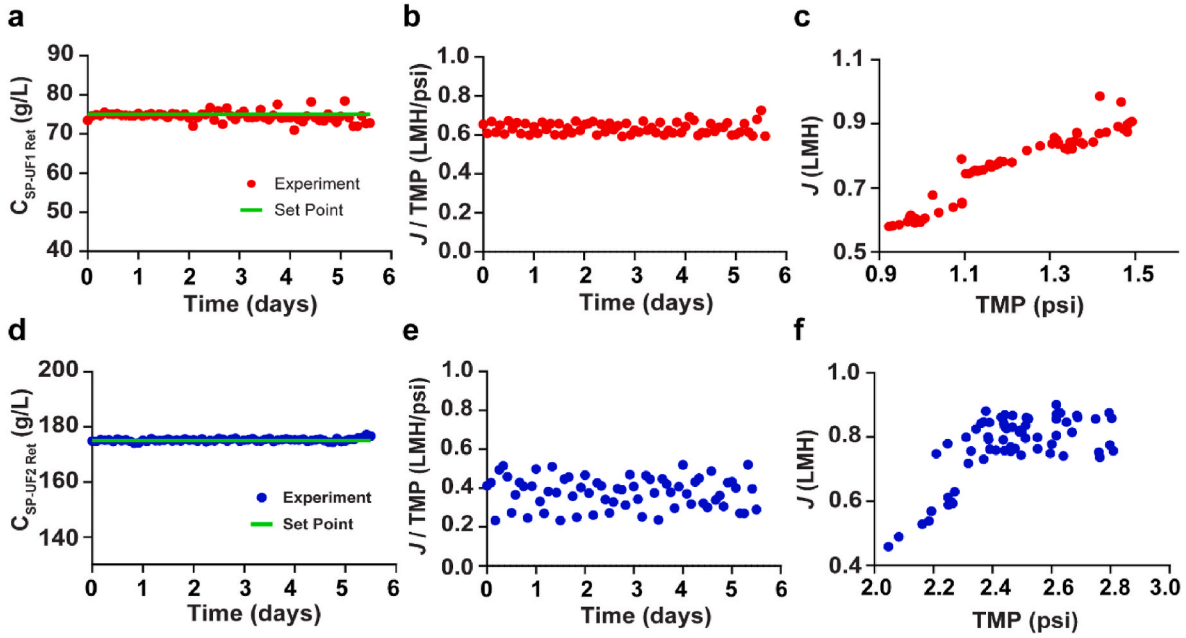

Fig. 9. Integrated and continuous SP-UF performance at the commercial scale. Plots of a) the retentate concentration over time, b) ratio of $J/\ TMP$ over time, and c) the permeate flux as a function of TMP for the SP-UF1 operation. Plots of d) the retentate concentration over time, e) ratio of J/TMP over time, and f) the permeate flux as a function of TMP for SP-UF2 operation.

The series configuration of the SP-UF1 filters allowed for maximum sweeping of the inlet stream thereby decreasing concentration polarization and fouling on the membrane surface as evidenced by a nearly constant J/TMP ratio of 0.6–0.7 LMH/psi (see Fig. 9b). The $J/$ TMP ratio is a measure of the inverse of filter resistance and is indicative of the presence of a constant gel layer that neither grows nor decays during the operation [43,59]. Furthermore, a linear increase in permeate flux with TMP (Fig. 9c) shows that the SP-UF1 operation performed as designed in the pressure-dependent regime. This linear increase confirms that the TMP was modulated automatically in response to fluctuations in the feed flowrate or feed concentration or both.

A similar performance was observed in the SP-UF2 operation wherein a mean feed concentration of 76.5 ± 0.8 g/L was concentrated ($C_{SP-UF2\ Ret}$) to 175.2 ± 0.5 g/L (setpoint of 175 g/L) over the same 6-day period (see Fig. 9d). Analogous to SP-UF1, a nearly constant $J/$ TMP ratio indicates the absence of any membrane fouling or concentration polarization (see Fig. 9e). It is interesting to note that this ratio is 0.23–0.52 LMH/psi, which is around 1.4–3.0 times smaller than that of SP-UF1. This lower ratio shows that the resistance is higher in SP-UF2 compared to SP-UF1, which is expected due to the relatively higher protein concentration of ~175 g/L. Additionally, the permeate flux increases with TMP up to a value of 2–2.3 psi. Beyond these values, TMP

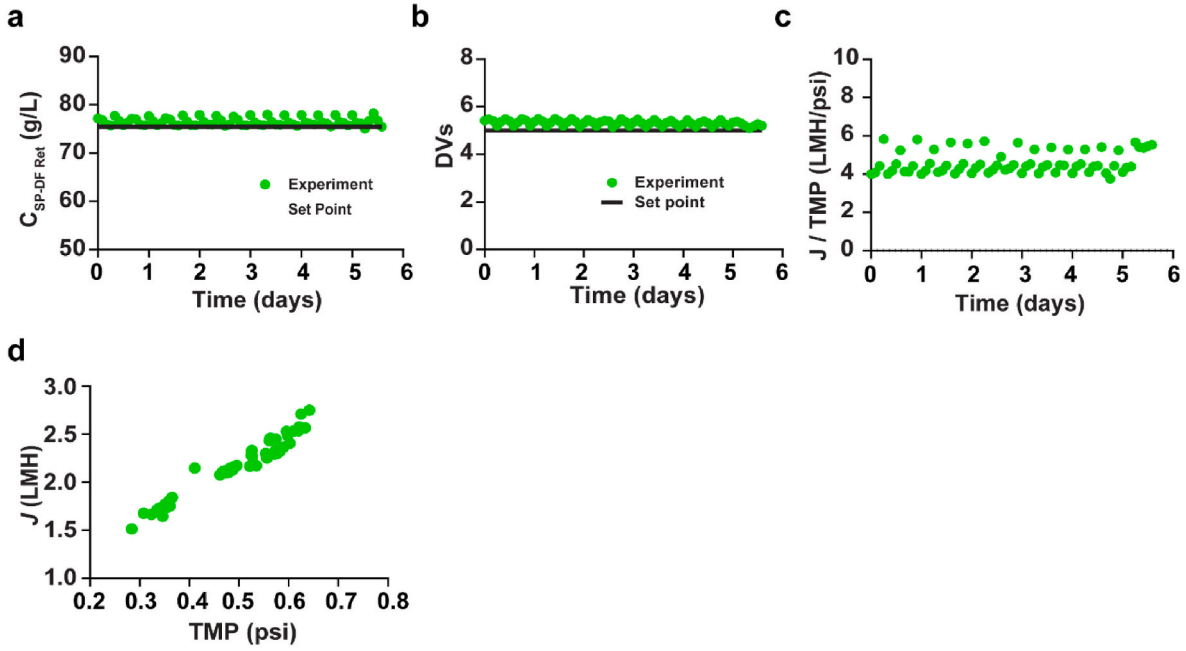

Fig. 10. Integrated and continuous SP-DF performance at the commercial scale. Plots of the a) diafiltered retentate concentration over time, b) achieved DVs, c) $J/$ TMP ratio over time, and the d) permeate flux as a function of TMP.

had a negligible impact on permeate flux (see Fig. 9f) suggesting the presence of a thicker gel layer due to the higher concentration and the lower feed flowrate. Additionally, the increase in viscosity with concentration (see Fig. S3) reduced the permeate flux causing the controller to frequently vary the TMP to achieve the required retentate concentration, which potentially caused the SP-UF2 operation to shift intermittently into the pressure-independent regime.

4.3.2. Integrated and continuous SP-DF

For SP-DF, both concentration (Fig. 5a) and buffer addition (Fig. 5b) controllers were implemented to maintain the retentate protein concentration ($C_{SP-DF\ Ret}$) and to achieve the targeted diavolumes. Specifically, the retentate concentration was maintained at 76.5 ± 0.8 g/L (same as the feed concentration of 74.5 ± 1.3 g/L) (Fig. 10a) and 5.3 ± 0.1 DVs (Fig. 10b) of buffer exchange was achieved for a setpoint of 5 DVs. As seen in the figure, the actual number of DVs achieved was always greater than the target value. This difference was primarily due to fluctuations (see Figs. S6a, S6b, and S6c) in the surge vessel prior to SP-UF1. Nevertheless, a constant J/TMP ratio between 3.7 and 5.8 LMH/psi confirms the absence of significant membrane fouling (Fig. 10c) as in SP-UF1 and SP-UF2. The permeate flux versus TMP profile (Fig. 10d) also shows that the SP-DF unit was operated in the pressure-dependent regime, which is the intended and optimal operating range in integrated and continuous SP-UF and SP-DF operations. Finally, it should be noted that the impact of the buffer excipients on Donnan effect was not studied as the DF buffer used, for the integrated operation, was previously optimized during batch process development.

To summarize, our results (SP-UF1/SP-UF2 and SP-DF) from the commercial scale integrated and continuous biomanufacturing demonstration clearly show the significant potential of the proposed SP-TFF operation. The novel PAT-based control strategy, developed in this work, uses a combination of process modeling, inline monitoring and control sensors, and a simple controller mechanism to monitor process parameters and maintain the product and process attributes at every step (i.e., SP-UF1, SP-DF, SP-UF2) of the SP-TFF process. As can be seen from Figs. 9 and 10 and **S4**, the main highlights of our work are consistent process control over 6 days of continuous and integrated SP-TFF operations, demonstrated by (1) consistent permeate flux and minimal membrane fouling (determined by a constant J/TMP ratio), (2) tight control of process parameters, including retentate concentration (within ~0.5–2.5% of target) and diavolumes (within ~8% of target) (see Table 3). These are crucial characteristics needed for successful implementation of any integrated and continuous SP-TFF operation for extended periods [45] and in fact, we have demonstrated the above characteristics at both low (SP-UF1, ~75 g/L) and high (SP-UF2, ~175 g/L) protein retentate concentrations (see Fig. 9), which showcases that our approach can be applied for a wide range of conditions.

Though integrated and continuous SP-TFF have been demonstrated in some prior works, they have generally been limited to ~12 h of continuous operation. Specifically, in those works, flow ratio controllers have been deployed to obtain a range of volumetric concentration factors (2–25x) [29,44]. Nevertheless, gradual membrane fouling and reduction of permeate flux have been observed at high retentate concentrations (~100 g/L) within ~9 h of operation, leading to intermediate cleaning and buffer wash cycles, and temporary pausing of continuous operation [44]. Thus, handling these situations would require either oversized surge vessels to collect material from the upstream process during the pause or a parallel SP-TFF module to continue processing [44], both of which are not ideal. For less stable intermediates, using oversized surge vessels would result in longer residence time distribution while adding a parallel SP-TFF module would add complexity in terms of operation, automation and costs [60]. As our approach prevents decline of permeate flux, any intermediate cleaning or buffer wash cycles are not necessary and thus, eliminates the need for intermediate oversized surge vessels or a parallel SP-TFF module. In another work [45], the achieved retentate concentration was within ±10% of its target (~40 g/L), which might be acceptable for lower retentate concentrations by absolute magnitude. However, a similar deviation at a higher retentate concentration scenario might result in out-of-specification batches, a case unlikely in our approach (±0.5% at 175 g/L).

5. Conclusion

In this work we have proposed a systematic approach which can be adopted to implement SP-TFF operations in the bioprocessing of therapeutics and validated it by demonstrating an integrated and continuous operation of SP-UF and SP-DF. Briefly, our systematic approach involved (1) conducting bench-scale experiments at potential operating conditions to characterize the SP-TFF process, (2) developing semi-empirical J_{max} models as a function of the feed flux and feed concentration for the operating ranges, (3) identifying the optimum filter sizing and SP-TFF performance, and (4) implementing robust process control to (i) achieve desired protein concentration in SP-UF, and (ii) maintain consistent concentration and obtain targeted DVs of buffer exchange in SP-DF. Our proposed technique can also be employed for batch SP-UF and SP-DF operations in a straightforward manner.

Our novel SP-TFF approach is the first of its kind to achieve (1) minimal membrane fouling, (2) consistent permeate flux, and (3) tight control of process parameters, including retentate concentration (within ~0.5–2.5% of target) and diavolumes (within ~8% of target) for 6 days of continuous and integrated SP-TFF operations. This is accomplished by leveraging inline concentration, flow sensors, and a back pressure regulator to actively control the SP-TFF process in the pressure-dependent regime of the permeate flux Vs TMP curve. Our generalized approach can be applied for modalities (e.g., fusion molecules, enzymes, etc.) other than mAbs as well. However, to develop understanding of the molecule and its impact on SP-UF and SP-DF operations (e.g., protein-membrane and protein-protein interactions), limited small-scale experiments are essential. Besides the above advantages, several opportunities for further improvement were also identified. As a substitute for PID controllers used in this work, model-predictive controllers, which are known to handle larger magnitudes of disturbances by prior training, could be employed.

To our knowledge, this is the first such work that has successfully integrated and demonstrated single-pass UF and single-pass DF in a continuous format. We believe that the ability to perform continuous SP-UF and SP-DF is one of the key elements that must be incorporated for the successful integrated and continuous biomanufacturing of formulated drug substance, a direction the entire pharmaceutical industry is moving towards.

CRediT author contribution statement

Shashi Malladi: Conceptualization, Methodology, Software, Formal Analysis, Investigation, Visualization, Writing – Original draft. **Michael J. Coolbaugh:** Conceptualization, Methodology, Software, Supervision, Writing – Review & Editing. **Crystal Thomas:** Methodology, Investigation. **Sushmitha Krishnan:** Methodology, Investigation. **Chad T. Varner:** Conceptualization, Writing – Review & Editing. **Jason Walther:** Conceptualization, Project administration, Funding acquisition, Writing – Review & Editing. **Kevin P. Brower:** Conceptualization, Funding acquisition, Writing – Review & Editing.

Declaration of competing interest

The authors declare the following financial interests/personal relationships which may be considered as potential competing interests: A patent application on the integrated and continuous SP-TFF technology.

Data availability

Data will be made available on request.

Acknowledgements

The authors would like to thank Alexander Helling and Martin Leuthold from Sartorius Stedium Biotech for providing the prototype SP-DF cassettes used in this work. The authors also acknowledge their upstream colleagues – Jeffrey Swana and Daryl Powers for execution of the 500L perfusion bioreactor for the commercial demonstration in this work. The authors also thank the automation team, especially Matthew Stundtner, Craig Williams, and Gavin Brown for the configuration and automation of all hardware and coding the control algorithms in DeltaV.

Appendix A. Supplementary data

Supplementary data to this article can be found online at https://doi.org/10.1016/j.memsci.2023.121633.

References

[1] K. Konstantinov, Towards Fully Continuous Bioprocessing: what Can We Learn from Pharma, Cell Culture Engineering XII, Banff, Canada, 2010, pp. 25–30.
[2] J.H. Vogel, H. Nguyen, M. Pritschet, R. Van Wegen, K. Konstantinov, Continuous annular chromatography: general characterization and application for the isolation of recombinant protein drugs, Biotechnol. Bioeng. 80 (5) (2002) 559–568, https://doi.org/10.1002/bit.10411.
[3] K.B. Konstantinov, C.L. Cooney, White paper on continuous bioprocessing may 20–21 2014 continuous manufacturing symposium, J. Pharmaceut. Sci. 104 (3) (2015) 813–820, https://doi.org/10.1002/jps.24268.
[4] R. Patil, J. Walther, Continuous manufacturing of recombinant therapeutic proteins: upstream and downstream technologies, Adv. Biochem. Eng. Biotechnol. 165 (2018) 277–322, https://doi.org/10.1007/10_2016_58.
[5] J. Walther, J. Lu, M. Hollenbach, M. Yu, C. Hwang, J. McLarty, K. Brower, Perfusion cell culture decreases process and product heterogeneity in a head-to-head comparison with fed-batch, Biotechnol. J. 14 (2) (2019), e1700733, https://doi.org/10.1002/biot.201700733.
[6] N. Gomez, J. Lull, X. Yang, Y. Wang, X. Zhang, A. Wieczorek, J. Harrahy, M. Pritchard, D.M. Cano, M. Shearer, C. Goudar, Improving product quality and productivity of bispecific molecules through the application of continuous perfusion principles, Biotechnol. Prog. 36 (4) (2020), e2973, https://doi.org/10.1002/btpr.2973.
[7] Y. Qin, R. Ma, Y. Li, Y. Li, G. Chen, W. Zhou, Productivity and quality improvement for a symmetric bispecific antibody through the application of intensified perfusion cell culture, Antib Ther 5 (2) (2022) 111–120, https://doi.org/10.1093/abt/tbac009.
[8] J. Xu, M.S. Rehmann, M. Xu, S. Zheng, C. Hill, Q. He, M.C. Borys, Z.J. Li, Development of an intensified fed-batch production platform with doubled titers using N-1 perfusion seed for cell culture manufacturing, Bioresour. Bioproces. 7 (1) (2020) 17, https://doi.org/10.1186/s40643-020-00304-y.
[9] A. Yongky, J. Xu, J. Tian, C. Oliveira, J. Zhao, K. McFarland, M.C. Borys, Z.J. Li, Process intensification in fed-batch production bioreactors using non-perfusion seed cultures, mAbs 11 (8) (2019) 1502–1514, https://doi.org/10.1080/19420862.2019.1652075.
[10] W.C. Yang, D.F. Minkler, R. Kshirsagar, T. Ryll, Y.M. Huang, Concentrated fed-batch cell culture increases manufacturing capacity without additional volumetric capacity, J. Biotechnol. 217 (2016) 1–11, https://doi.org/10.1016/j.jbiotec.2015.10.009.
[11] Y.M. Huang, W. Hu, E. Rustandi, K. Chang, H. Yusuf-Makagiansar, T. Ryll, Maximizing productivity of CHO cell-based fed-batch culture using chemically defined media conditions and typical manufacturing equipment, Biotechnol. Prog. 26 (5) (2010) 1400–1410, https://doi.org/10.1002/btpr.436.
[12] J. Walther, R. Godawat, C. Hwang, Y. Abe, A. Sinclair, K. Konstantinov, The business impact of an integrated continuous biomanufacturing platform for recombinant protein production, J. Biotechnol. 213 (2015) 3–12, https://doi.org/10.1016/j.jbiotec.2015.05.010.
[13] J. Pollock, J. Coffman, S.V. Ho, S.S. Farid, Integrated continuous bioprocessing: economic, operational, and environmental feasibility for clinical and commercial antibody manufacture, Biotechnol. Prog. 33 (4) (2017) 854–866, https://doi.org/10.1002/btpr.2492.
[14] H. Mahal, H. Branton, S.S. Farid, End-to-end continuous bioprocessing: impact on facility design, cost of goods, and cost of development for monoclonal antibodies, Biotechnol. Bioeng. 118 (9) (2021) 3468–3485, https://doi.org/10.1002/bit.27774.
[15] V. Warikoo, R. Godawat, K. Brower, S. Jain, D. Cummings, E. Simons, T. Johnson, J. Walther, M. Yu, B. Wright, J. McLarty, K.P. Karey, C. Hwang, W. Zhou, F. Riske, K. Konstantinov, Integrated continuous production of recombinant therapeutic proteins, Biotechnol. Bioeng. 109 (12) (2012) 3018–3029, https://doi.org/10.1002/bit.24584.
[16] T.C. Silva, M. Eppink, M. Ottens, Automation and miniaturization: enabling tools for fast, high-throughput process development in integrated continuous biomanufacturing, J. Appl. Chem. Biotechnol. 97 (9) (2022) 2365–2375, https://doi.org/10.1002/jctb.6792.
[17] V. Chopda, A. Gyorgypal, O. Yang, R. Singh, R. Ramachandran, H. Zhang, G. Tsilomelekis, S.P.S. Chundawat, M.G. Ierapetritou, Recent advances in integrated process analytical techniques, modeling, and control strategies to enable continuous biomanufacturing of monoclonal antibodies, J. Appl. Chem. Biotechnol. 97 (9) (2022) 2317–2335, https://doi.org/10.1002/jctb.6765.
[18] A.S. Rathore, S. Nikita, G. Thakur, N. Deore, Challenges in process control for continuous processing for production of monoclonal antibody products, Curr. Opinion Chem. Eng. 31 (2021), 100671, https://doi.org/10.1016/j.coche.2021.100671.
[19] R. Godawat, K. Brower, S. Jain, K. Konstantinov, F. Riske, V. Warikoo, Periodic counter-current chromatography – design and operational considerations for integrated and continuous purification of proteins, Biotechnol. J. 7 (12) (2012) 1496–1508, https://doi.org/10.1002/biot.201200068.
[20] J. Pollock, G. Bolton, J. Coffman, S.V. Ho, D.G. Bracewell, S.S. Farid, Optimising the design and operation of semi-continuous affinity chromatography for clinical and commercial manufacture, J. Chromatogr. A 1284 (2013) 17–27, https://doi.org/10.1016/j.chroma.2013.01.082.
[21] M.R. Brown, R. Orozco, J. Coffman, Leveraging flow mechanics to determine critical process and scaling parameters in a continuous viral inactivation reactor, Biotechnol. Bioeng. 117 (3) (2020) 637–645, https://doi.org/10.1002/bit.27223.
[22] L. David, M.P. Bayer, M. Lobedann, G. Schembecker, Simulation of continuous low pH viral inactivation inside a coiled flow inverter, Biotechnol. Bioeng. 117 (4) (2020) 1048–1062, https://doi.org/10.1002/bit.27255.
[23] C.A. Teske, B. Lebreton, R. van Reis, Inline ultrafiltration, Biotechnol. Prog. 26 (4) (2010) 1068–1072, https://doi.org/10.1002/btpr.404.
[24] A.M.K. Nambiar, Y. Li, A.L. Zydney, Countercurrent staged diafiltration for formulation of high value proteins, Biotechnol. Bioeng. 115 (1) (2018) 139–144, https://doi.org/10.1002/bit.26441.
[25] A. Brinkmann, S. Elouafiq, J. Pieracci, M. Westoby, Leveraging single-pass tangential flow filtration to enable decoupling of upstream and downstream monoclonal antibody processing, Biotechnol. Prog. 34 (2) (2018) 405–411, https://doi.org/10.1002/btpr.2601.
[26] J. Dizon-Maspat, J. Bourret, A. D'Agostini, F. Li, Single pass tangential flow filtration to debottleneck downstream processing for therapeutic antibody production, Biotechnol. Bioeng. 109 (4) (2012) 962–970, https://doi.org/10.1002/bit.24377.
[27] M.C. Flickinger, S.W. Drew, Encyclopedia of Bioprocess Technology: Fermentation, Biocatalysis, and Bioseparation, John Wiley, 1999.
[28] M.W. Paper, Single-pass Tangential Flow Filtration, a Versatile Application to Streamline Biomanufacturing, 2018.
[29] C. Casey, T. Gallos, Y. Alekseev, E. Ayturk, S. Pearl, Protein concentration with single-pass tangential flow filtration (SPTFF), J. Membr. Sci. 384 (1-2) (2011) 82–88.
[30] A. Arunkumar, N. Singh, M. Peck, M.C. Borys, Z.J. Li, Investigation of single-pass tangential flow filtration (SPTFF) as an inline concentration step for cell culture harvest, J. Membr. Sci. 524 (2017) 20–32.
[31] C. Casey, K. Rogler, X. Gjoka, R. Gantier, E. Ayturk, CadenceTM single-pass TFF coupled with chromatography steps enables continuous bioprocessing while reducing processing times and volumes, Pall Scientific (2018).
[32] A.L. Zydney, Perspectives on integrated continuous bioprocessing—opportunities and challenges, Curr. Opinion Chem. Eng. 10 (2015) 8–13, https://doi.org/10.1016/j.coche.2015.07.005.
[33] M.J. Coolbaugh, C.T. Varner, T.A. Vetter, E.K. Davenport, B. Bouchard, M. Fiadeiro, N. Tugcu, J. Walther, R. Patil, K. Brower, Pilot-scale demonstration of an end-to-end integrated and continuous biomanufacturing process, Biotechnol. Bioeng. 118 (9) (2021) 3287–3301, https://doi.org/10.1002/bit.27670.
[34] A. Jungbauer, Continuous downstream processing of biopharmaceuticals, Trends Biotechnol. 31 (8) (2013) 479–492, https://doi.org/10.1016/j.tibtech.2013.05.011.
[35] M.G. Jabra, A.M. Lipinski, A.L. Zydney, Single pass tangential flow filtration (SPTFF) of monoclonal antibodies: experimental studies and theoretical analysis, J. Membr. Sci. 637 (2021), 119606, https://doi.org/10.1016/j.memsci.2021.119606.
[36] R. Campos, Cadence single-pass TFF coupled with chromatography steps enables continuous bioprocessing while reducing processing times and volumes, Pall Scientific (2018).
[37] J. Rucker-Pezzini, L. Arnold, K. Hill-Byrne, T. Sharp, M. Avazhanskiy, C. Forespring, Single pass diafiltration integrated into a fully continuous mAb purification process, Biotechnol. Bioeng. 115 (8) (2018) 1949–1957, https://doi.org/10.1002/bit.26708.
[38] R. Tan, M. Franzreb, Continuous ultrafiltration/diafiltration using a 3D-printed two membrane single pass module, Biotechnol. Bioeng. 117 (3) (2020) 654–661, https://doi.org/10.1002/bit.27233.
[39] C.J. Yehl, A.L. Zydney, Single-use, single-pass tangential flow filtration using low-cost hollow fiber modules, J. Membr. Sci. 595 (2020), 117517, https://doi.org/10.1016/j.memsci.2019.117517.
[40] J. Kaiser, J. Krarup, E.B. Hansen, M. Pinelo, U. Krühne, Defining the optimal operating conditions and configuration of a single-pass tangential flow filtration (SPTFF) system via CFD modelling, Sep. Purif. Technol. 290 (2022), 120776, https://doi.org/10.1016/j.seppur.2022.120776.

[41] G. Thakur, A.S. Rathore, Modelling and optimization of single-pass tangential flow ultrafiltration for continuous manufacturing of monoclonal antibodies, Sep. Purif. Technol. 276 (2021), 119341.
[42] M. Huter, J. Strube, Model-based optimization of SPTFF ultrafiltration for integration in continuous biopharmaceutical processing, Chem. Ing. Tech. 90 (2018), https://doi.org/10.1002/cite.201855263, 1251-1251.
[43] E. Binabaji, J. Ma, S. Rao, A.L. Zydney, Theoretical analysis of the ultrafiltration behavior of highly concentrated protein solutions, J. Membr. Sci. 494 (2015) 216–223, https://doi.org/10.1016/j.memsci.2015.07.068.
[44] G. Thakur, S. Thori, A.S. Rathore, Implementing PAT for single-pass tangential flow ultrafiltration for continuous manufacturing of monoclonal antibodies, J. Membr. Sci. 613 (2020), 118492, https://doi.org/10.1016/j.memsci.2020.118492.
[45] G. Thakur, V. Masampally, A. Kulkarni, A.S. Rathore, Process analytical technology (PAT) implementation for membrane operations in continuous manufacturing of mAbs: model-based control of single-pass tangential flow ultrafiltration, AAPS J. 24 (4) (2022) 83, https://doi.org/10.1208/s12248-022-00731-z.
[46] J.L. Nilsson, Protein fouling of uf membranes: causes and consequences, J. Membr. Sci. 52 (2) (1990) 121–142, https://doi.org/10.1016/S0376-7388(00)80481-0.
[47] E. Binabaji, S. Rao, A.L. Zydney, The osmotic pressure of highly concentrated monoclonal antibody solutions: effect of solution conditions, Biotechnol. Bioeng. 111 (3) (2014) 529–536, https://doi.org/10.1002/bit.25104.
[48] P. Schausberger, N. Norazman, H. Li, V. Chen, A. Friedl, Simulation of protein ultrafiltration using CFD: comparison of concentration polarisation and fouling effects with filtration and protein adsorption experiments, J. Membr. Sci. 337 (1) (2009) 1–8, https://doi.org/10.1016/j.memsci.2009.03.022.
[49] P. Corporation, Pellicon 3 Cassettes with Ultracel® Membrane Performance Guide, 2018.
[50] A.R. Da Costa, A.G. Fane, D.E. Wiley, Spacer characterization and pressure drop modelling in spacer-filled channels for ultrafiltration, J. Membr. Sci. 87 (1) (1994) 79–98, https://doi.org/10.1016/0376-7388(93)E0076-P.
[51] L.J. Zeman, A.L. Zydney, Microfiltration and Ultrafiltration - Principles and Applications, Marcel Dekker, New York, 1996, https://doi.org/10.1002/cite.330691022. New York, 1997.
[52] EmdMillipore, Optimization and Process Simulation for Ultrafiltration.
[53] A. Suki, A.G. Fane, C.J.D. Fell, Flux decline in protein ultrafiltration, J. Membr. Sci. 21 (3) (1984) 269–283, https://doi.org/10.1016/S0376-7388(00)80218-5.
[54] G.B. van den Berg, C.A. Smolders, Flux decline in ultrafiltration processes, Desalination 77 (1990) 101–133, https://doi.org/10.1016/0011-9164(90)85023-4.
[55] G.D.L. Reyes, L. Mir, Method and Apparatus for the Filtration of Biological Solutions, 2008.
[56] E. Madsen, J. Kaiser, U. Krühne, M. Pinelo, Single pass tangential flow filtration: critical operational variables, fouling, and main current applications, Sep. Purif. Technol. 291 (2022), 120949, https://doi.org/10.1016/j.seppur.2022.120949.
[57] D. Zhang, P. Patel, D. Strauss, X. Qian, S. Ranil Wickramasinghe, Modeling tangential flow filtration using reverse asymmetric membranes for bioreactor harvesting, Biotechnol. Prog. 37 (1) (2021), e3084, https://doi.org/10.1002/btpr.3084.
[58] Millipore, Protein Concentration and Diafiltration by Tangential Flow Filtration.
[59] Z. He, D.J. Miller, S. Kasemset, D.R. Paul, B.D. Freeman, The effect of permeate flux on membrane fouling during microfiltration of oily water, J. Membr. Sci. 525 (2017) 25–34, https://doi.org/10.1016/j.memsci.2016.10.002.
[60] M. Krippl, T. Kargl, M. Duerkop, A. Dürauer, Hybrid modeling reduces experimental effort to predict performance of serial and parallel single-pass tangential flow filtration, Sep. Purif. Technol. 276 (2021), 119277, https://doi.org/10.1016/j.seppur.2021.119277.